LETTER

Low and increased solubility of silicon in metal nitrides: evidence by X-ray absorption near edge structure

Jose Luis Endrino · Sergio Palacín ·
Alejandro Gutiérrez · Franz Schäffers ·
James E. Krzanowski

Adding silicon to transition metal nitride (MN) films has been reported to significantly improve many of their mechanical properties including hardness, toughness, and oxidation resistance [1, 2]. As a result, the influence of microstructure on the mechanical properties of silicon-containing metal nitrides has been a subject of intensive investigation for more than a decade [3]. Most microstructural studies of these materials report the formation of two-phase nanocomposite systems composed of nanocrystalline (nc) metal nitride grains embedded in an amorphous silicon nitride (a-Si:N) matrix [2]. This formation of nanocomposite microstructures has been explained by the lower free energy of the separate phases in comparison to that of ternary or quaternary nitride compounds. It has been argued that because the phase segregation rate is diffusion-controlled, temperatures above 500 °C are needed in order to constrain any solubility of silicon into the metal nitride [4]. This claim has been supported, in most cases, using X-ray Diffraction (XRD)
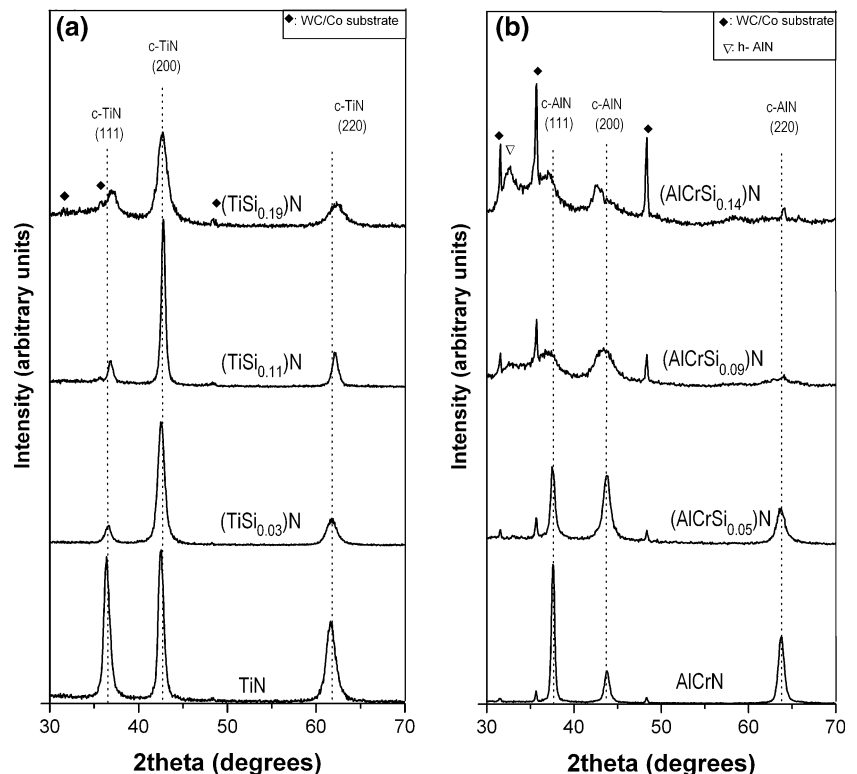
J. L. Endrino
Instituto de Ciencia de Materiales de Madrid, Consejo Superior de Investigaciones Científicas, Cantoblanco, Madrid 28049, Spain

S. Palacín · A. Gutiérrez (✉)
Física Aplicada, Facultad de Ciencias, Universidad Autonoma de Madrid, Ctra Colmenar km 15, Cantoblanco, Madrid 28049, Spain
e-mail: a.gutierrez@uam.es

F. Schäffers
BESSY GmbH, Albert-Einstein-Strasse 15, Berlin 12489, Germany

J. E. Krzanowski
Department of Mechanical Engineering, University of New Hampshire, Durham, NH 03824, USA

and transmission Electron Microscopy (TEM) techniques. These techniques are limited and cannot prove phase segregation has actually occurred during the deposition of the film or during sample preparation. However, recently, few studies have laid out the possibility of small amounts of Si dissolution into MN grains using X-ray absorption spectroscopy techniques [5, 6].

This work reports on the local structure and bonds of silicon in TiSiN and AlCrSiN investigated by X-ray diffraction (XRD) and X-ray absorption near edge structure (XANES). Samples were deposited using pulsed magnetron sputtering from Ti and Si targets and cathodic arc evaporation from customized AlCrSi targets, which contained 70 at.% of Al and a variable amount of Cr and Si, respectively. Both systems were deposited at 500 °C. Mirror-polished squared cemented carbide inserts were used as substrates. The thickness of all the coating samples was within 3.5 ± 0.2 μm. A Siemens D500 diffractometer with a CuKα tube and the Θ/2Θ mode was used to perform XRD analysis and identify the phases formed. Chemical analysis was performed using Electron Dispersive Spectroscopy (EDS). XANES measurements of the Ti and Si K-edges were carried out at the KMC-1 beamline of the BESSY synchrotron facility with double crystal monochromator using a standard chamber equipped with a high-resolution solid-state fluorescence detector. Si (111) monochromator crystals were used to provide photon energy selection at the Cr K-edge and Ti-Kedge while InSb (111) was used to collect the Si K-edge spectra.

In Fig. 1a, x-ray diffraction patterns for TiSiN films revealed the formation of polycrystalline films containing the B1-TiN phase [7]. Increase in Si content resulted in a preferential growth change to (200) and a slight shift of the diffraction peaks to larger 2-theta. This shift suggests a small contraction of the NaCl type-TiN lattice with the

Fig. 1 X-ray diffraction patterns for deposited coatings with increasing silicon content; vertical lines are associated with the unalloyed cubic phase. (**a**) TiSiN. (**b**) AlCrSiN

presence of Si, perhaps due to a small incorporation of Si in the lattice and the formation of short Ti-Si bonds. In the case of the sample with the highest Si content (19 at.%), the broadening of the peaks suggests a strong loss of crystallinity of the material. In comparison, Fig. 1b shows the XRD patterns for the AlCrSiN samples. In the case of the Si-free AlCrN and the sample with 5 rel. at.% of Si, the peaks fell between those for B1-aluminum nitride [8] and B1-chromium nitride [9], suggesting that in these two cases, there is a complete solubility of chromium, aluminum and nitrogen in the rock-salt type lattice and silicon does not interact. The two samples that contained larger amounts of silicon, showed amorphous peaks at the positions marked as cubic AlN (111) and (200) planes. In these samples, the XRD pattern shows a shift of the cubic peaks towards lower angles and the presence of a peak at $2\Theta \sim 32.3$ degrees which can be consistent with the (001) hexagonal plane for wurtzite hcp-AlN [10].

Figure 2a shows XANES spectra at the Ti K-edge of TiSiN samples with different Si content. In this case, all spectra keep a similar lineshape to that of titanium nitride, independently of Si content. The pre-edge region, which is associated to transitions from Ti-1s states to Ti-3d states hybridized with Si-2p states, does not show significant changes with Si-addition. This suggests a weak interaction between Ti and Si. Figure 2b shows XANES spectra at the Cr K-edge of AlCrSiN with different Si content. Similarly, the pre-edge region, at 5960 eV, is associated with transi-
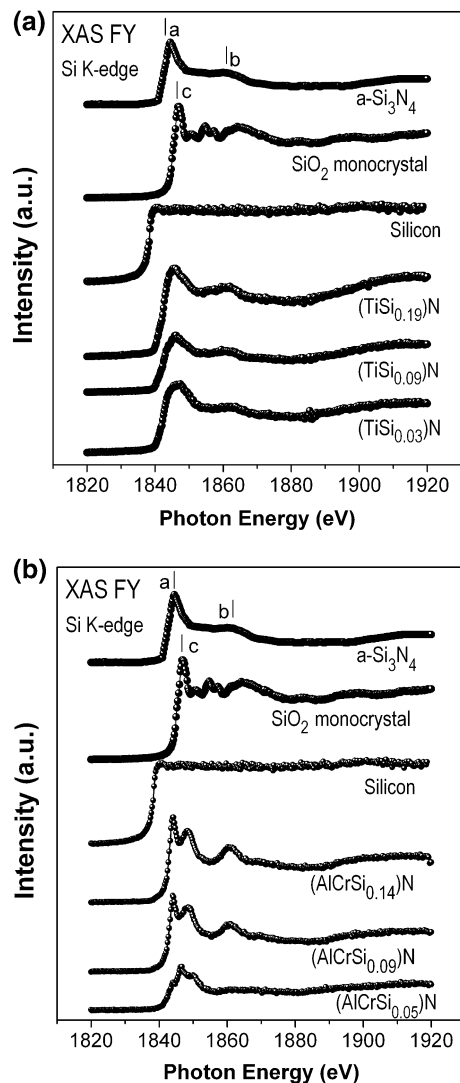
tions from Cr-1s states to Cr-3d states hybridized with 2p empty states of the ligand atoms. This hybridization allows 1s-3d transitions, which are otherwise dipole forbidden. The spectrum for the AlCrN sample shows only a tiny pre-edge peak at this position, very similar to that reported in previous works for Cr_2O_3 [11–13], suggesting that Cr in this compound is in the form of Cr3+. The intensity of this peak slightly increases for sample with a Si content of 5%. For samples with even higher Si content, the intensity increase is still more predominant. The increase of this feature could be explained in the case of oxide compounds in terms of a valence increase from +3 to +4, +5 or +6, or in terms of a reduction of crystalline domains down to the nanoscale [12]. We do not have evidence of nanocrystalline domains formation and, on the other hand, the presence of high valence Cr would involve a shift to higher energies of the main absorption edge, which is not observed in our samples, so the presence of this kind of Cr compounds can be excluded [13]. To explain the observed intensity increase in our samples, the chemical interaction between Si and Cr, which would give rise to Cr-3d Si-2p hybridization, must be taken into account. Consequently, the peak at 5960 eV can be assigned to transitions from Cr-1s states to Cr-3d states hybridized with Si-2p empty states. Additionally to this pre-edge intensity increase, the addition of Si produces a smoothening of the overall spectral lineshape, which is commonly associated with an amorphization of
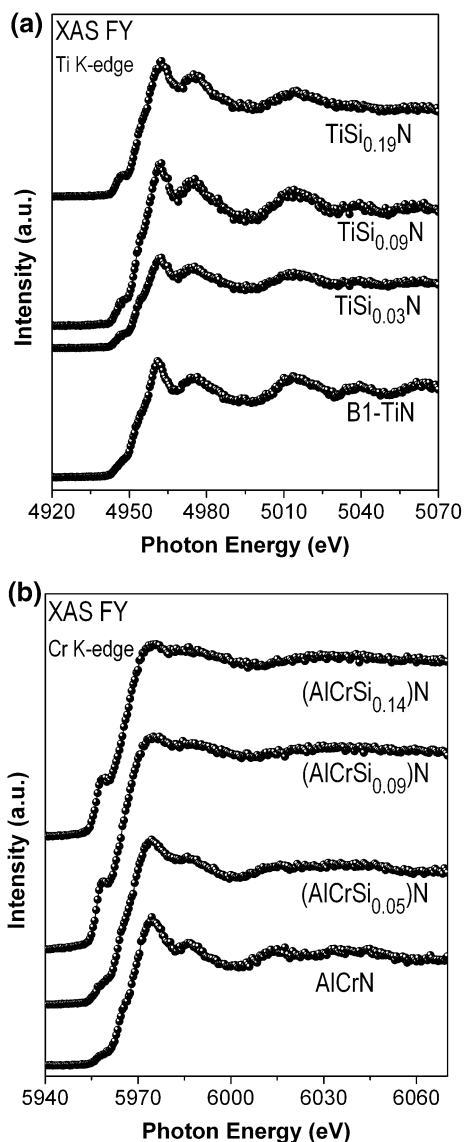
Fig. 2 X-ray absorption near edge structure (XANES) spectra in fluorescence yield mode. (a) Ti K-edge. (b) Cr K-edge

Fig. 3 Silicon K-edge XANES spectra in fluorescence yield mode for deposited coatings. (a) TiSiN. (b) AlCrSiN. In addition, reference spectra for Si, SiO_2, and a-Si_3N_4 are shown

the microstructure [14], and is consistent with that observed by XRD.

Figure 3a shows XANES spectra at the Si K-edge of TiSiN samples with different Si content, as well as pure Si and SiO_2 single crystals, and an amorphous Si_3N_4 as reference samples for comparison. As can be observed by comparing the top spectrum with all TiSiN spectra, in all cases the spectral lineshape is typical of Si_3N_4. Features a and b of the top spectrum, typical of Si_3N_4, were present in all TiSiN samples, and there was not any significant change with silicon content. Figure 3b shows XANES spectra at the Si K-edge of AlCrSiN samples with different Si content, as well as pure Si and SiO_2 single crystals, and an amorphous Si_3N_4 as reference samples for comparison. From a comparison of the AlCrSiN spectra with that of

pure Si, we can exclude that Si incorporates to the lattice as an atomic solid solution, because then the spectra would resemble that of pure Si. The spectrum for sample with 5 at.% Si (bottom), has a peak at 1847 eV, which is aligned with feature c of the spectrum for SiO_2 single crystal. This would suggest the presence of oxygen contamination for low Si content, probably in the form of SiO_2. Additionally, the edge positions at 1842 eV, as well as the small shoulder observed at 1845 eV, at the same position of feature a of the top spectrum, are evidences for the presence of Si-N compounds in this sample. The feature assigned to SiO_2 disappears for samples with higher Si content. The spectra for samples with 9 and 14 at.% of Si are very similar, with a main peak at 1844 eV. This energy position corresponds to the main peak observed for Si_3N_4, suggesting that Si is in the form of some nitride compound. However, the more

complex spectral lineshape as compared to that of Si_3N_4, could be an evidence of the formation of some ternary Si-N-X compound.

In summary, the present comparative work reports evidence of both reduced and increased silicon solubility for samples prepared at a high deposition temperature. In the TiSiN system, we have observed features corresponding to a-Si_3N_4 in all of the deposited samples and there was not any significant change with silicon content. Both Ti-K and Si-K spectra suggests that there was a weak interaction between Ti and Si. Whereas for the quaternary AlCrSiN system, there was strong evidence of the formation of Si-N-X complex compounds, where X could account for Cr, Al, or both. Samples also showed the amorphization of the Cr-based crystal structure with increasing Si content.

References

1. Beake BD, Vishnkayov VM, Vallizadeh R, Collignon JS (2006) J Phys D: Appl Phys 39:1392
2. Zeman P, Musil J (2006) Appl Surf Sci 252:8319
3. Vêrprek S, Reiprich S (1995) Thin Solid Films 268:64
4. Vaz F, Rebouta L, Goudeau Ph, Girardeau T, Pacaud J, Riviére JP, Traverse A (2001) Surf Coat Technol 146–147:274
5. Meng WJ, Zhang XD, Shi B, Jiang JC, Rehn LE, Baldo PM, Tittsworth RC (2003) Surf Coat Technol 163–164:251
6. Zhang XD, Meng WJ, Wang W, Rehn LE, Baldo PM, Evans RD (2004) Surf Coat Technol 177–178:325
7. Joint Committee Powder Diffraction Standard (JCPDS) Card No. 38-1420
8. Joint Committee Powder Diffraction Standard (JCPDS) Card No. 24-1495
9. Joint Committee Powder Diffraction Standard (JCPDS) Card No. 11-0065
10. Joint Committee Powder Diffraction Standard (JCPDS) Card No. 08-0262
11. Berry J (2004) Amer Mineralogist 89:790
12. Pantelouris A, Modrow H, Pantelouris M, Hormes J, Reinen D (2004) Chem Phys 300:13
13. Hwang S-J, Park H-S, Choy J-H (2002) Solid State Ionics 151:275
14. Gutiérrez A, López MF, Hernando A, Rojo JM (1997) Phys Rev B 56:5039